Journal of Geochemical Exploration 158 (2015) 22–33

Contents lists available at ScienceDirect

Journal of Geochemical Exploration

journal homepage: www.elsevier.com/locate/jgeoexp

Geochemistry of serpentine agricultural soil and associated groundwater chemistry and vegetation in the area of Atalanti, Greece

Christos Kanellopoulos [a,*], Ariadne Argyraki [b], Panagiotis Mitropoulos [b]

[a] Section of Earth and Environmental Studies, University of Geneva, Rue des Maraîchers 13, 1205 Geneva, Switzerland
[b] Faculty of Geology and Geoenvironment, University of Athens, Panepistimioupoli Zografou, 157 84 Athens, Greece

ARTICLE INFO

Article history:
Received 13 November 2014
Revised 11 May 2015
Accepted 28 June 2015
Available online 2 July 2015

Keywords:
Ni contamination
Cr contamination
Weathering
Geochemical mapping
Serpentine agricultural soil

ABSTRACT

The soil geochemistry was studied in the area of Atalanti, Greece, an area characterized by presence of mafic and ultramafic rock members of an ophiolite complex. The objectives of the study were to evaluate their impact on soil chemistry and to establish the geochemical baseline of soil with respect to elements derived from the ophiolite rocks. A total of 118 agricultural soil samples were collected and found to be enriched in Ca (7.6%), Co (31 mg/kg), Cr (230 mg/kg), Cu (37 mg/kg), Mg (2.9%) and Ni (330 mg/kg) relative to the median values of both European and Greek soils. Soil baseline concentrations of the ophiolite derived elements (Cr, Ni, Co) were estimated within two sub-areas and the variation in their concentration was assessed along two toposequences characterized by different intensities of weathering of parent rock. Differences in groundwater chemistry were also demonstrated for the aquifers developing within the two subareas. The results of this study can be utilized in future studies on serpentine soil in temperate climate by providing an objective basis for setting realistic threshold values for pollution assessment and remediation.

1. Introduction

The term "serpentine soils" is used to describe any soil derived from ultramafic rock or serpentinite (metamorphosed ultramafic rock). Although these rocks and soils cover minimal area of the earth's surface, they are present in populated areas within the Circum-Pacific margin and the Mediterranean (Oze et al., 2004a). The study of such areas is of particular interest to environmental geochemistry because soil, groundwater and sometimes vegetation near ultramafic rocks are known to contain high concentrations of potentially harmful elements (PHEs) including Cr, Ni, Co and Mn (Brooks, 1987; Cheng et al., 2011; Gasser and Dahlgren, 1994; Gough et al., 1989; Kabata-Pendias and Mukherjee, 2007; Oze et al., 2004a,b, 2008).

Due to the wide geographical occurrence and distribution of serpentinites and serpentine soils, weathering processes differ from location to location due to varying climatic conditions and nature of the parent material as well as other factors including topography, biota, time and tectonic activity (Chardot et al., 2007; Garnier et al., 2013; Hseu and Iizuka, 2013; Proctor and Nagy, 1992; Sadegh et al., 2012). As a result, the chemistry of these soils, groundwater and vegetation will differ from site to site and might represent, in varying degree, a geogenic source of elements with possible health implications for humans (Cox et al., 2013; Kabata-Pendias and Mukherjee, 2007; Kelepertzis and Stathopoulou, 2013; Selinus et al., 2005). Ranges in natural geochemical variability combined with bioaccessibility and ecotoxicological studies may then provide an objective basis for setting appropriate risk-related regulatory levels in such areas.

In Greece, mafic and ultramafic rocks of ophiolitic sequences cover large areas (Pe-Piper and Piper, 2002). This is reflected on the elevated geochemical background of Cr, Ni and Co in soil observed over the whole country in the FOREGS (Salminen et al., 2005) and GEMAS (Reimann et al., 2014) Geochemical Atlases of Europe. Studies have been conducted in order to estimate the impact of PHEs from the ultramafic rocks on soil and water (Kelepertzis et al., 2013; Megremi, 2010; Megremi et al., 2012; Vardaki and Kelepertsis, 1999), the environmental availability of these geogenic elements in affected areas (Economou-Eliopoulos et al., 2011; Kelepertzis and Stathopoulou, 2013; Megremi, 2010) and baseline soil mapping of such areas (Kanellopoulos and Argyraki, 2013). Recent publications on Cr(VI) contaminated areas (Dermatas et al., 2012; Economou-Eliopoulos et al., 2011; Moraetis et al., 2012) highlight even more the need of establishing such baselines in order to provide an objective basis for decision making and selection of appropriate mitigation measures.

This paper presents the results of a soil geochemical survey in the agricultural area of Atalanti, central Greece, which is characterized by outcropping ultramafic rocks and genetically related agricultural alluvial soil. The objectives of the study were: (a) to evaluate the impact of ultramafic rocks on soil chemistry including groundwater chemistry

* Corresponding author.
E-mail addresses: ckanellopoulos@gmail.com (C. Kanellopoulos), eargyraki@geol.uoa.gr (A. Argyraki), pmitrop@geol.uoa.gr (P. Mitropoulos).

http://dx.doi.org/10.1016/j.gexplo.2015.06.013
0375-6742/

and characteristic annual plant species as ancillary data and (b) to establish the local geochemical baseline of soil with respect to geogenic elements derived from the ultramafic rocks.

2. Study area

2.1. Geographical location and land use

The study area is located in central Greece between latitudes 38° 69′ and 38° 55′ and longitudes 22° 97′ and 23° 08′ and covers 64 km^2 (Fig. 1). Its topography is characterized by an alluvial valley, opening to the sea on the east, surrounded by rocky mountains on the south and west. Intensive agricultural activities take place in the area while some livestock farming and small industrial units also exist. Atalanti town with population of ~6000, is located on the western part of the study area.

2.2. Geological setting

The studied area geologically belongs to the sub-Pelagonian geotectonic unit (Jolivet et al., 2013; Mountrakis, 1986). The Valley of Atalanti consists of post-Alpine deposits (Fig. 1) comprising mainly Quaternary-alluvial sediments, consisting of weathered material from the surrounding hills. Neogene lacustrine sediments including marl, clay, gravel, sandstone, conglomerate and marly limestone outcrop in the periphery of the valley. Rocky mountains to the south of the valley are composed of Cretaceous flysch, comprised of shale, sandstone, conglomerate and intercalated limestone; Cretaceous limestone and a shale-chert formation. Serpentinized peridotite, dolerite and gabbro are found within this layer. The rocks from the ophiolitic sequence in the area also outcrop south of the valley at higher topographic locations, near the village of Kirtoni. They comprise mostly ultramafic rocks consisting of peridotite, dunite, pyroxene–peridotite and olivinite. The degree of serpentinization varies from slight alteration to complete serpentinization (IGME, 1965). Diabase, dolerite, igneous basic tuff, pillow lava and spilite are also present towards the lower topographic parts. The ophiolitic rocks are tectonically overthrusted on Jurassic carbonate and clastic rocks, also intercalated by ophiolites. Weathered peridotite also outcrops on the north-northwest of the alluvial valley. The Chlomo Mountain, rising on the south west of the alluvial valley is built of Triassic compacted dolomite. Permo-carboniferous layers occur on the southwest part of the valley, near Atalanti town. This volcanic–clastic formation consists of graywacke, conglomerate, quartzite, violet shale, marly sandstone, green keratophyric tuff and thin layers of dark limestone.

2.3. Soil description

The soil type within the valley is Calcaric reflecting the composition of the surrounding mountains which are built mostly of carbonate rocks. However, samples collected near ultramafic rocks are characterized as Chromic. Calcaric Fluvisols develop in the central and eastern parts of Atalanti Valley. In the mountainous southern part of the studied area the soil horizon is usually shallow (Calcaric and Chromic Leptosols). Chromic Luvisols, enriched in clay and iron-bearing minerals appear on the south-western edge of Atalanti Valley, NW of Megaplatanos.

3. Materials and methods

3.1. Soil sampling and analysis

A total of 118 soil samples were collected from 64 sites in the field (Fig. 1). A sampling grid of 1 × 1 km covered the area within the Atalanti Valley. Additional samples were collected along a north–south transect extending south of the valley up to Kirtoni area, cutting through the mafic and ultramafic rocks that appear in higher elevation. This allowed the study of elemental variation in the shoulder, backslope and footslope along the toposequence.

At each sampling site, the surface of the soil was cleared of superficial debris, vegetation and the O-soil horizon material before taking a 3 fold composite sample using an Edelman type hand auger. Sixty four soil samples were collected from a 0–25 cm depth and 54 samples were collected at a depth of 25–50 cm wherever this was possible.

After collection, the samples were dried in an oven at a temperature of 40 °C, disaggregated with a porcelain pestle and mortar and sieved through nylon screens of 2 mm. The finer fraction (<2 mm) was homogenized and pulverized to <0.075 mm in an agate mill. Soil samples were digested with a mixture of $HClO_4$–HNO_3–HCl acids and were analyzed for a series of elements by inductively coupled plasma-atomic emission spectroscopy (ICP-AES, Vista-PRO Simultaneous) at the Natural History Museum of London, UK and by inductively coupled plasma-mass spectrometry (ICP-MS, Agilent 7500ce) at the Department of Biology and Environmental Science, University of Sussex, UK. It should be noted that perchloric–nitric–hydrochloric is a partial extraction method and is not very effective on spinels (e.g., chromite) or ilmenite, leading to underestimation of total Cr, Ti, V and other resistant mineral associated elements. Analytical data quality was assured by introduction of internal standards, use of certified (NIST SRM 2709, 2710, 2711) and house reference material samples in randomized positions within the analytical batch and by blank and duplicate analysis of a proportion of the samples (Ramsey et al., 1987). Analytical bias and precision were subsequently calculated and found to be within acceptable limits (<10%) for the following elements: Al, As, Ba, Ca, Cd, Co, Cr, Cu, Fe, K, Mg, Mn, Ni, Pb, Se, Sr, Ti, U, V, and Zn. Thus, data analysis and interpretation was focused on this group of elements.

The soil mineralogy was studied in order to explore the relationship between the source (parent rock) of inorganic compounds and their weathering products within the soil matrix. The mineralogical composition of soil was investigated by powder X-ray diffraction (XRD) and microprobe analysis. The XRD study was carried out at the Laboratory of Economic Geology and Geochemistry, University of Athens using a Siemens 5005 X-ray diffractometer, operating with Cu Ka radiation at 40 kV, 40 nA, 0.020° step size and 1.0 s step time. Soil samples were finely ground in an agate mortar and pressed into pellets for XRD analysis. The XRD patterns were evaluated using the EVA 2.2 program of the Siemens DIFFRAC and the D5005 software package.

Polished sections were prepared by impregnating soil in epoxy resin, and examined by reflected light microscopy and scanning electron microscopy–energy dispersive spectroscopy (SEM–EDS). Microprobe analyses and SEM imaging were carried out at the Laboratory of Economic Geology and Geochemistry, University of Athens, using a JEOL JSM 5600 scanning electron microscope, equipped with an automated energy dispersive analysis system ISIS 300 OXFORD, with the following operating conditions: accelerating voltage 20 kV, beam current 0.5 nA, time of measurement 50 s and beam diameter 1–2 mm. The spectra were processed using the ZAF program (3 iterations).

3.2. Groundwater sampling and analysis

A total of 13 groundwater samples were collected from wells, springs and boreholes used for urban water supply or for agricultural activities (Fig. 1). Unstable parameters including pH, temperature, electrical conductivity, and total dissolved solids were measured in the field, using portable apparatus. For the chemical analysis, the samples were collected in polyethylene bottles. 1 L of sample was vacuum-filtered through 0.45 μm pore size membrane filters and stored in a polyethylene container. Another 200 mL portion of each sample was vacuum-filtered with the same membrane filters and acidified to a final concentration of about 2% nitric acid and stored in a polyethylene container. All samples were preserved in a refrigerator.

Sulfate, nitrate, phosphate and chloride were measured spectrophotometrically, using a Hach DR/2000 apparatus. Bicarbonate was measured

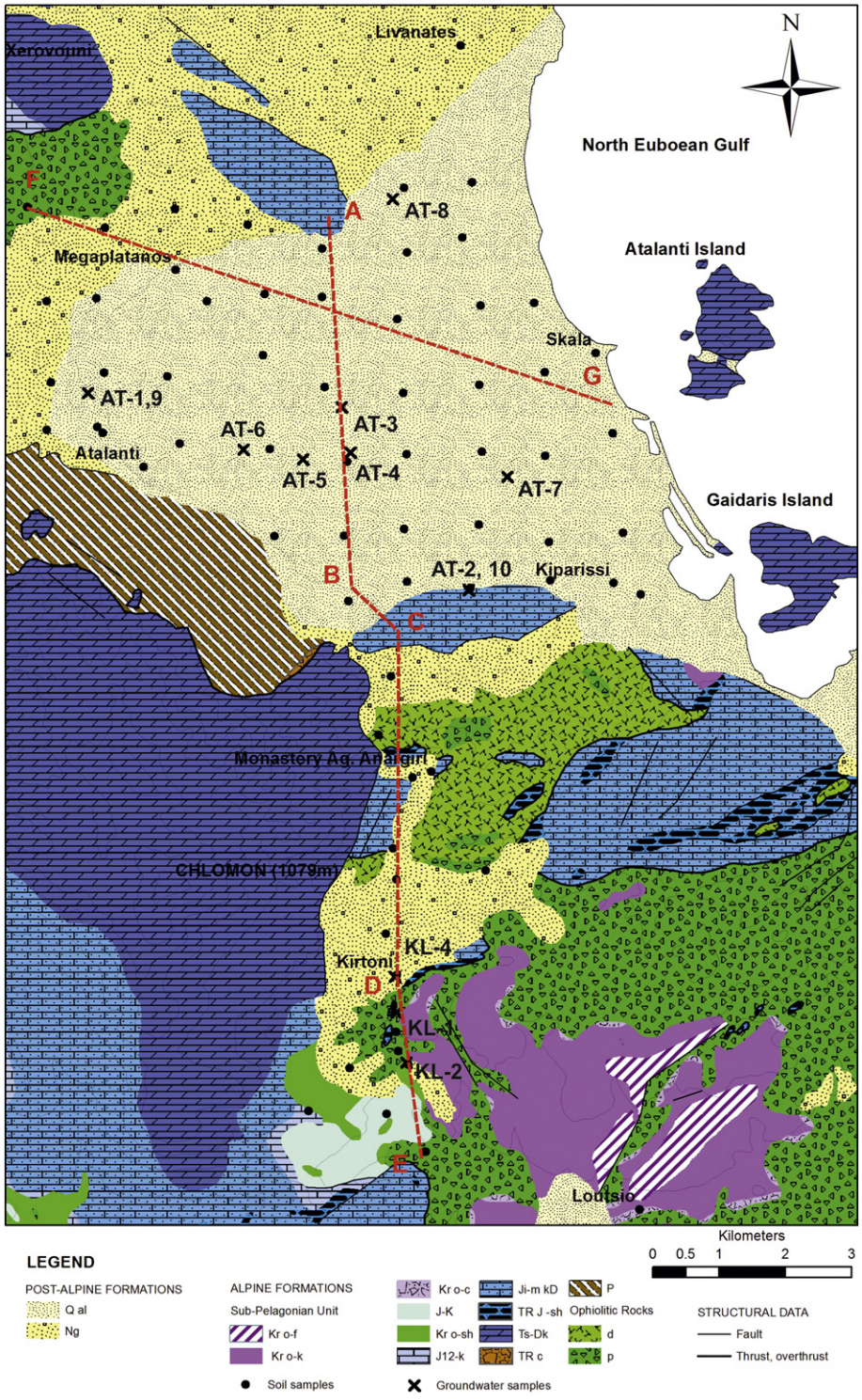

Fig. 1. Geological map of the study area. Qal = alluvial deposits, Ng = Neogene deposits, Kr o-f = Upper Cretaceous flysch, Kr o-k = Upper Cretaceous transgressive limestone, Kr o-c = conglomerates of the Upper Cretaceous, J–K = Lower Cretaceous limestones, Kr-o sh = Cretaceous to Kimmeridgian shale–chert formation, which also contain limestones and serpentinized peridotite, dolerite and gabbros, J12-k = Upper Jurassic limestones, Ji-m kD = Middle and Lower Jurassic limestones, TR J-sh = Middle to Lower Jurassic shale-chert formation, which also contain limestones, intercalated by ophiolites and their tuffs and serpentinites, and Ts-Dk = Upper–Middle Triassic. Compacted dolomites, TR-c = conglomerate of the transgression of the Triassic system of layers (Permo-carboniferous elements such as gravels of keratophyre, of graywackes, of sandstones, of schists, of black limestones), P = Permo-carboniferous layers (graywackes, conglomerates, quartzites, violet shales, marly sandstones, green keratophyric tuffs), d = diabase–dolerite, and p = peridotite, dunite, pyroxene peridotite, and olivinite.

using a Hach alkalinity titrator. Sodium and K were measured using a flame photometer, Jenway PFP 7. Metals Cd, Co, Cr, Mn, Pb, Ni, Fe, Zn, Ca, and Mn were analyzed using atomic absorption spectrometer (AAS), Perkin Elmer model 1100B, with Graphite Furnace (HGA-400). In cases of high concentrations of the previous elements and for Ca and Mn, flame atomic absorption spectrometer (F-AAS) was used. All of the above analyses were conducted at the Laboratory of Economic Geology and Geochemistry, University of Athens. Furthermore, selected samples

were analyzed by inductively coupled plasma-mass spectrometry (ICP-MS) at the ACME Analytical Laboratories Ltd., Canada, for a series of 70 elements.

3.3. Statistical analysis and use of GIS

The correlation matrix of the studied elements was computed for the two subareas of Atalanti and Kirtoni after normalization of the variables by transforming the arithmetic values to their logarithms. This transformation was necessary in order to fulfill the assumption of normality in the application of parametric statistical tests. Furthermore, the medians of elemental concentrations in the two subareas were compared by using the non-parametric Mann–Whitney test.

ArcGIS 9.3 was used to create a simplified digital geological map showing the main lithological types that appear in the studied area. This map was based on published geological map (IGME, 1965) of scale 1:50,000 as well as updated, detailed geological maps. A spatial database was developed in ArcGIS and elemental concentrations were linked to the sampling points. The interpolated surface of concentrations was plotted showing the major spatial trends within the alluvial plain. Concentration class intervals were selected on the basis of the statistical distribution for each element using the 'natural breaks' method. Graduated symbols over the actual sampling sites were also plotted based on quartiles of the statistical distribution of concentration values.

4. Results

4.1. Soil mineralogy

The results of XRD mineralogical study for selected samples are presented in Table 1. The XRD spectrum of the soil samples showed the presence of serpentine and smectite. The existence of smectite was evidenced by the characteristic expansion of peak from 15 Å to 18 Å after glycolation (Fig. S1, Supplementary material).

Selected microphotographs of soil grains and microanalysis data are presented in Fig. 2 and Table S1(Supplementary material).

Common soil mineralogical phases comprising mainly quartz, albite, clay minerals, iron oxides, Ca-amphibole and serpentine minerals were determined in nearly all studied samples. Dolomite and in some cases calcite was identified in soil samples located near carbonate rocks, e.g.,Chlomo Mountain which consists mostly of dolomite.

In addition, detailed study of the samples using SEM–EDS indicated the presence of characteristic mineral phases related to the mineralogical composition of neighboring rock exposures at different locations. Soil samples from Kirtoni were characterized by the presence of chromite (Cr_2O_3 ~ 33–63%), chlorite or Cr-rich (Cr_2O_3 ~ 2.5%) chlorite and magnetite or Cr-rich magnetite (Cr_2O_3 ~ 1%) (Fig. 2, Table S1). Soil samples from the Kirtoni area contain abundant clastic grains of large, angular, chromite, or rounded Cr-rich magnetite (Cr_2O_3 ~ 1–2%) (Fig. 2C, D). These minerals are derived from the weathering processes of ultramafic rocks within the ophiolitic sequence (Kanellopoulos, 2011) and are a typical source of Cr in soil (Garnier et al., 2008). The soil samples from Atalanti contain minerals of the spinel group, small grains of chromite, simple or Cr-rich magnetite (Cr_2O_3 ~ 1%) with exsolusion of ilmenite (TiO_2 2–9%), epidote (pumpellyite MgO 2–6%) and dolomite. All of the above are indicative of more intense weathering in the alluvial environment of Atalanti Valley, yet retaining the ultramafic geochemical signature reflected on Cr-rich soil grains.

It is noted that ultramafic rocks in the area consist mostly of serpentinized harzburgite and to a lesser extent dunite. Chromite inside unweathered ultramafic rocks appears in angular shaped crystals, scattered within harzburgite and dunite (Pomonis, 2015, personal comm.). Garnier et al. (2008) have reported changes in the morphology of chromite crystals in soil profiles at Niquelândia, Brazil during weathering and transformation from angular crystals to rounded shaped grains. Furthermore, in Cyprus soils from areas with high total Cr concentrations most of the Cr is bound up in resistant chromite in either clasts of transported ultramafics or as chromite in the heavy mineral-rich coastal sands (Cohen et al., 2012).

4.2. Chemical composition of soil

The statistical summary of the analytical results of soil samples is presented in Table 2 along with median values of elemental concentrations in soil reported in the Geochemical Atlas of Europe (Salminen et al., 2005) for the whole continent and Greece. With respect to median values, samples from the present study are enriched in As (11 mg/kg), Ca (7.6%), Co (31 mg/kg), Cr (230 mg/kg), Cu (37 mg/kg), Mg (2.9%) and Ni (330 mg/kg) exceeding the median values of both European and Greek soils. All elements demonstrated positively skewed distributions.

The correlation coefficients between elements related with ultramafic rocks like Co, Cr, Fe, and Ni are very strong (>0.8) in Kirtoni area (Table 3), while in Atalanti the same correlation coefficients are lower. The negative correlation coefficient of −0.81 between Ca and Fe in Atalanti is indicative of the various origins of material within the alluvial plain, i.e., Ca is enriched in soil due to limestone from Chlomo Mountain and Fe originates from the ultramafics mostly from Kirtoni. Also, the results of Mann–Whitney test show that the median values of all ophiolite derived elements except Mg, i.e., Ca, Co, Ni, Cr, Fe, and Mn, are statistically significantly different between the two sub-areas ($p < 0.05$).

Correlation coefficients between samples from the surface and deep soil horizon for the elements As, Ba, Ca, Co, Cr, Fe, Mg, Mn, Ni, Pb, and Ti

Table 1
Summary results of soil mineralogy in the study area according to X-ray diffraction.

Locality	Samples	Qtz	Cal	Dol	Ank	Feldspar		Ca-amphiboles		Fe-oxides			Ilt	Sme Gr	Clc	Tlc	Group of serpentine	
						Ab	Mc	Act	Tr	Mgh	Mag	Hem					Cctl	Lz
Atalanti	AT-1A-E	***	**	*		**		**	**	*	**	*	*	**	**	**	**	**
Atalanti	AT-1A-B	***				**		**	**	*	**	**	*	**	*	**	**	**
Atalanti	AT-4A-E	***		***		**		**	**	*	**	**	*	**			**	**
Atalanti	AT-4A-B	***		***	**	*		*	*	*	**	**	*	**			**	**
Atalanti	AT-5B-E	***	*	***	**	**		**	**	*	**	**	**	**	*	*	**	**
Atalanti	AT-5B-B	***		***	**	***		*	*	**	*	**	**	**	*		*	**
Atalanti	AT-5D-E	***	***	***	**	***		*	*	**	*	*	**	**	**	*	**	**
Atalanti	AT-5D-B	***	***	***	*	***		*	*	*	**	**	**	**	*	*	**	**
Kyrtoni	KL-7-E	***		*		*		**	**	*	**	*	**	**	*	*	**	**
Kyrtoni	KL-7-B	***		*		**		*	*	**	**	**	*	**		**	**	**
Kyrtoni	KL-9-E	***	***	*		*		*	*	**	**	**	**	**	**		**	**

Abbreviations: Qzt (quartz), Cal (calcite), Dol (dolomite), Ank (ankerite), Ab (albite), Mc (microcline), Act (actinolite), Tr (tremolite), Mgh (maghemite), Mag (magnetite), Hem (hematite), Ilt (illite), Sme Gr (smectice group), Clc (clinochlore), Tlc (talc), Cctl (clinochrysotile), and Lz(lizardite).
*** abundant, ** moderate, * minor or trace.

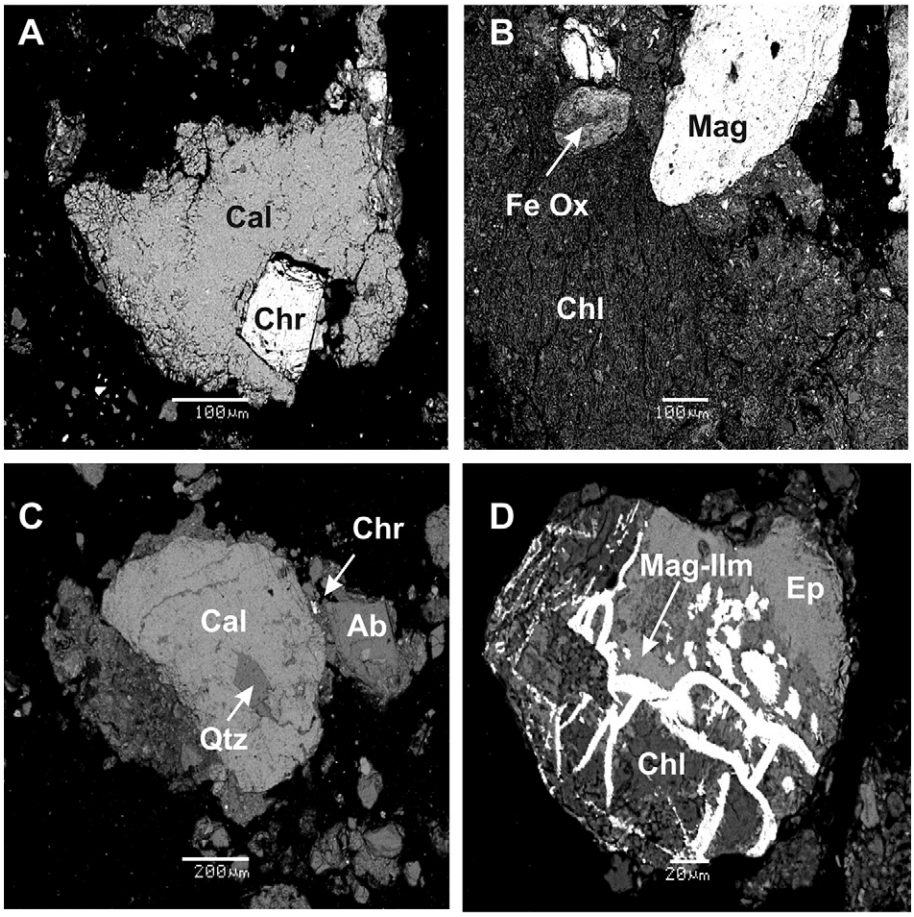

Fig. 2. Microphotographs in SEM-backscatter mode of mineral phases in soil samples. (A), (B): Kirtoni area — near ultramafic rocks, (C), (D): Atalanti area. (Abbreviations: Ab = albite, Ep = epidote, Cal = calcite, Chl = chlorite, Chr = chromite, Fe Ox = iron oxides, Ilm = ilmenite, Mag = magnetite, and Qtz = quartz).

were over 0.7 ($p < 0.05$), with highest values for Ba (0.9), Co (0.9), Cr (0.9), Mn (0.9), Ni (0.9), and Ti (0.9) suggesting geogenic origin of the elements (Fig. 3).

4.3. Spatial distribution of elements in soil

The geochemical maps of the studied elements are presented in Fig. 4.

Large occurrences of ultramafic rocks of the ophiolitic sequence, outcropping in the southern part of the study area (Kirtoni area) control the spatial distribution of Co, Cr, Fe, Mn and Ni. The above elements have maximum concentrations of 250 mg/kg, 4290 mg/kg, 14.45%, 3010 mg/kg, and 2730 mg/kg for Co, Cr, Fe, Mn and Ni respectively in Kirtoni area. Occurrences of volcanic–clastic formations, outcropping near the town of Atalanti area control the spatial distribution of Cu, Zn, and Ti. The highest concentrations of Cu, Zn and Ti are 676 mg/kg, 215 mg/kg and 2630 mg/kg respectively. However, high concentrations of Zn appear in soil samples near the occurrences of ultramafic rocks (Kirtoni area) (max 105 mg/kg). Probably the volcanic–clastic formation is the main source of Zn, Cu and Ti as their concentrations fall with relatively high rate, as we move away from the boundaries of the formation. A reason could be that the gentle slopes in this part of the study area do not favor intense physical weathering and soil grain transport downhill. Another group of elements including Ba, K, Sr and Ca is characterized by maximum concentrations, in both soil horizons, south of the limestone occurrence near Livanates village. The highest values of Ba (280 mg/kg), K (16,300 mg/kg), Sr (230 mg/kg) and Ca (31%) are found in the calcareous soil collected on Neogene formations in the NW edge of the study area at the foothill of Profitis Ilias (NE of Megaplatanos).

4.4. Water chemistry

In order to explore relationships between groundwater content and soil geochemistry, the results of chemical analysis were evaluated mainly in terms of PHE and major ion concentrations (Table 4). Two distinct aquifers exist within the study area: one, developing within the alluvial sediments of Atalanti Valley and another developing within marly limestone and conglomerate, uphill in Kirtoni. The lithology in both aquifers is characterized by the presence of fragments of ultramafic rock. Classification of the water samples according to their major aqueous species content was assessed by plotting the major ion concentrations on a Piper diagram revealing two distinct water types; samples from Atalanti Valley are classified as Mg–HCO_3 indicating a higher degree of serpentinization and samples around Kirtoni are classified as Ca–HCO_3 (Kanellopoulos et al., 2014). The distribution of the samples on the Mg–Ca–Na + K ternary diagram involving the four major cations combined with the Mg vs Ca plot (Fig. 5) reflect the interaction of groundwater with ultramafic rocks in Atalanti area (Garrels, 1968; Langone et al., 2013). Differently, Kitroni groundwater samples are in the Ca field, indicating a Ca–HCO_3 composition where Ca is controlled by the dissolution of Ca-rich phases. Furthermore, groundwater samples from Atalanti Valley present high concentrations of Cr (up to 25 μg/L), Fe (up to 270 μg/L), Mn (up to 5 μg/L), Mg (up to 60 μg/L) and Zn (up to 32 μg/L), while only one of the samples from Kirtoni presents high concentration of Ni (15 μg/L) (Table 4).

Table 2
Summary statistics of analyzed elements in top-soil samples (0–25 cm) in mg/kg (or %) for the total study area and for defined subareas of different controlling geologies. Upper baseline concentrations corresponding to threshold values (TH) with respective data percentiles are also presented for each sub-area.

	All samples (N = 64)								Greek soil[a] (N = 41)	European soil[a] (N = 843)
	Mean	Median	SD	Range	Min	Max	TH	Perc.	Median	Median
Al (%)	3.73	3.66	1.32	6.79	0.27	7.06	5.5	91	7.11	5.82
Ca (%)	8.36	7.67	5.93	30.81	0.22	31.03	16.9	92.5	1.62	0.659
Fe (%)	4.47	3.95	2.02	13.11	1.34	14.45	7.4	92.5	5.11	3.16
K (%)	0.63	0.59	0.04	1.61	0.02	1.63	1	92	1.44	1.59
Mg (%)	3.73	2.93	3.88	25.09	0.68	25.78	9.4	93	1.04	0.464
As	11	11	6	31	0.61	31	19	93	7	7
Ba	126	128	50	252	3	255	195	91.5	286	375
Co	43	31	39	235	10	245	100	93	21	8
Cr	453	234	753	4270	18	4290	1570	93	22	60
Cu	51	36	82	664	11	676	185	94	30	13
Mn	941	823	476	2730	275	3000	1640	93	891	503
Ni	533	334	672	2680	44	2730	1470	92	92	18
Pb	15	13	7	48	0.8	48	26	94	22	23
Se	7	7	4	14	2.7	17	14	91	–	–
Sr	73	72	36	190	0	190	124	92	94	89
Ti	1090	1030	567	2610	23	2630	1890	92	3820	3430
U	0.58	0.49	0.29	1.31	0	1.34	1	91	1.9	2
V	56	57	19	120	9	129	84	93	106	60
Zn	70	66	33	197	18	215	119	93	77	52

	Atalanti samples (N = 47)								Kirtoni samples (N = 17)							
	Mean	Median	SD	Range	Min	Max	TH	Perc.	Mean	Median	SD	Range	Min	Max	TH	Perc.
Al (%)	3.77	3.56	1.26	5.64	1.41	7.06	5.4	91	3.63	3.84	1.51	5.41	0.27	5.67	5.56	90
Ca (%)	9.66	8.23	5.71	29.40	1.64	31.03	17.7	92	4.76	2.33	5.13	17.94	0.22	18.2	11.8	91.5
Fe (%)	3.85	3.82	1.06	5.50	1.34	6.84	5.3	91.5	6.21	5.26	2.93	12.00	2.45	14.5	10.2	91.5
K (%)	0.64	0.64	0.18	0.82	0.26	1.08	0.88	91	0.60	0.48	0.46	1.61	0.02	1.63	1.2	91
Mg (%)	3.32	3.11	1.85	8.88	0.68	9.56	5.9	92	4.86	2.41	6.89	25.08	0.7	25.8	14.4	92
As	11	11	5	24	4	28	18	92	10	11	8	31	0.61	31	21	92
Ba	133	131	45	184	71	255	194	91.5	105	103	60	201	3	204	184	90.5
Co	28	30	7	30	10	40	39	90	84	72	59	226	18	245	165	91.5
Cr	213	194	155	739	29	768	436	92.5	1116	541	1235	4271	18	4290	2800	91.5
Cu	54	36	94	664	11.3	676	205	94	42	35	24	78	11	89	75	90
Mn	787	784	193	987	275	1260	1050	91	1370	1210	721	2540	465	3000	2290	90
Ni	260	276	140	435	44	478	431	89	1290	960	949	2620	105	2730	2500	90
Pb	16	13	7	40	8	48	26	92.5	13	13	8	28	0.84	29	23	90.5
Se	7	7	4	14	3	17	14	90.5	6	6	4	10	2.72	12	12	90
Sr	86	75	28	150	40	190	126	92.5	39	31	32	130	0.0025	130	83	91
Ti	1254	1139	536	2240	391	2630	1990	91.5	652	596	399	1620	23	1640	1180	90.5
U	0.6	0.6	0.3	1.1	0.2	1.3	1	91	0.4	0.36	0.3	1.3	0.03	1.3	0.8	92
V	57	57	16	74	20	94	77	91	55	54	27	120	9	129	92	91.5
Zn	68	65	31	197	18	215	116	93.5	77	72	37	148	18	166	127	91

SD = standard deviation, BS = upper baseline value, Perc. = percentile.
[a] Data used for the Geochemical Atlas of Europe.

Table 3
Correlation matrix of log-transformed elemental concentrations for Atalanti and Kirtoni top-soil samples.

	Ca	Co	Cr	Fe	Mg	Ni	Ti	V
Atalanti area								
Ca	1							
Co	−0.55	1						
Cr	−0.18	0.25	1					
Fe	**−0.81**	0.62	−0.16	1				
Mg	0.11	0.00	−0.40	−0.09	1			
Ni	−0.02	0.65	0.56	−0.01	0.02	1		
Ti	−0.69	0.20	−0.28	0.72	0.20	−0.45	1	
V	−0.73	0.27	−0.14	**0.84**	−0.08	−0.35	**0.86**	1
Kirtoni area								
Ca	1							
Co	0.01	1						
Cr	0.08	**0.93**	1					
Fe	−0.02	**0.93**	**0.89**	1				
Mg	−0.39	0.47	0.32	0.32	1			
Ni	−0.08	**0.93**	**0.91**	**0.83**	0.47	1		
Ti	0.02	−0.54	−0.50	−0.35	−0.29	−0.61	1	
V	0.16	0.37	0.54	0.55	−0.35	0.23	0.20	1

Bold values indicate significance at $p < 0.05$.

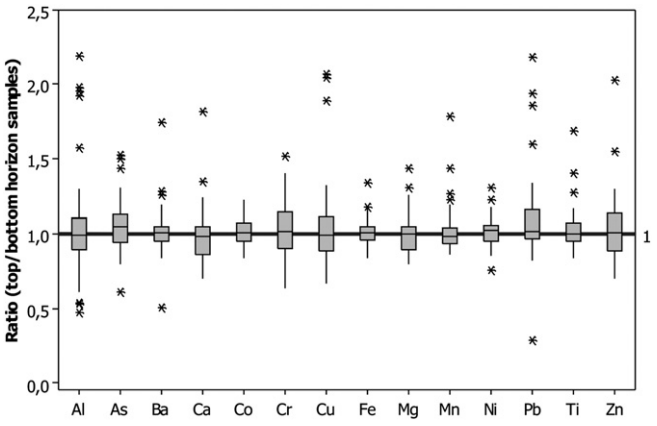

Fig. 3. Box-plots comparing elemental concentration ratios of top (0–25 cm) and bottom (25–50 cm) soil horizons in the study area.

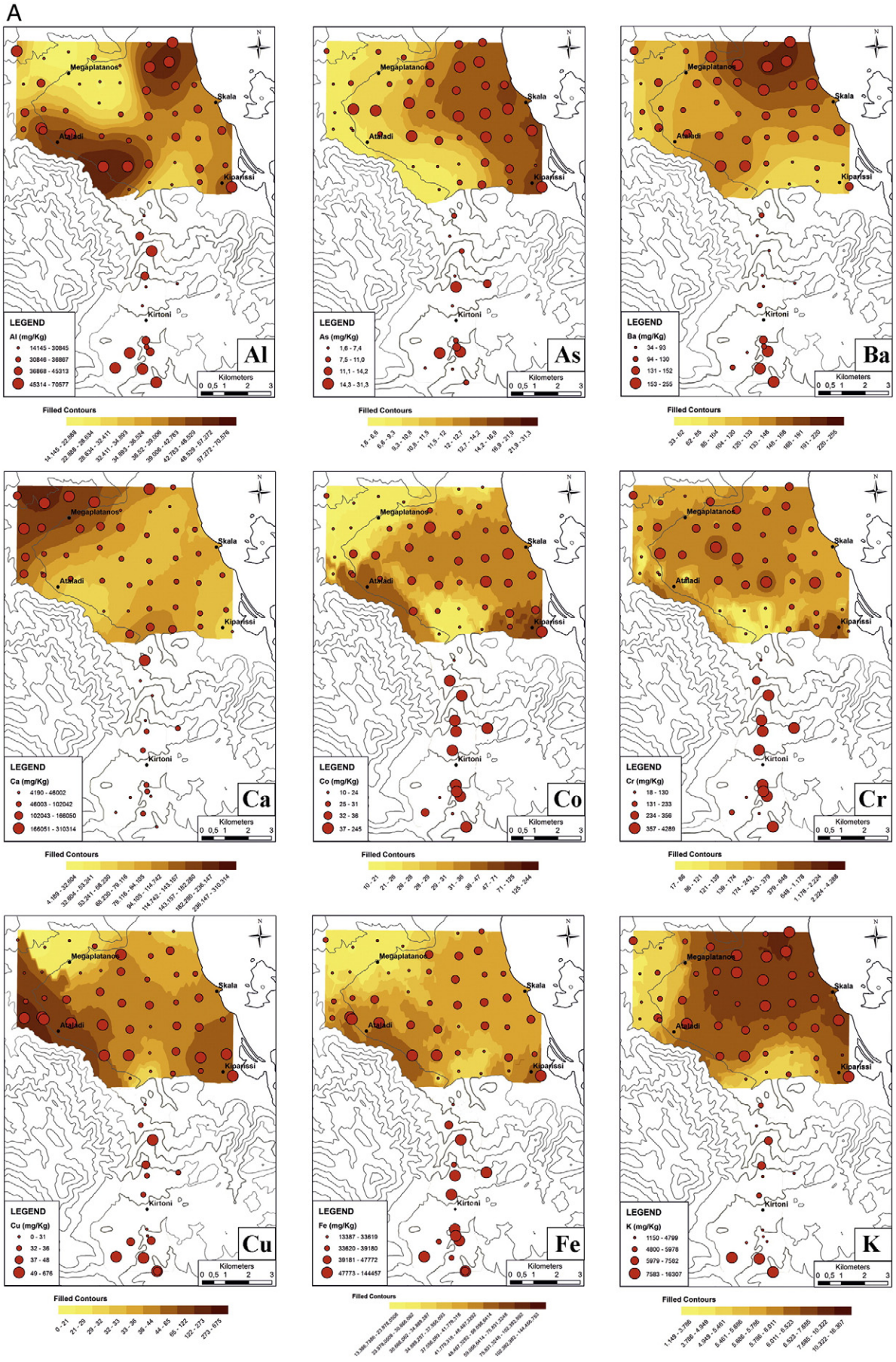

Fig. 4. Geochemical maps of the study area showing distribution of Al, As, Ba, Ca, Co, Cr, Cu, Fe, K, Mg, Mn, Ni, Pb, Sr, Ti, U, V, and Zn in top soil.

B

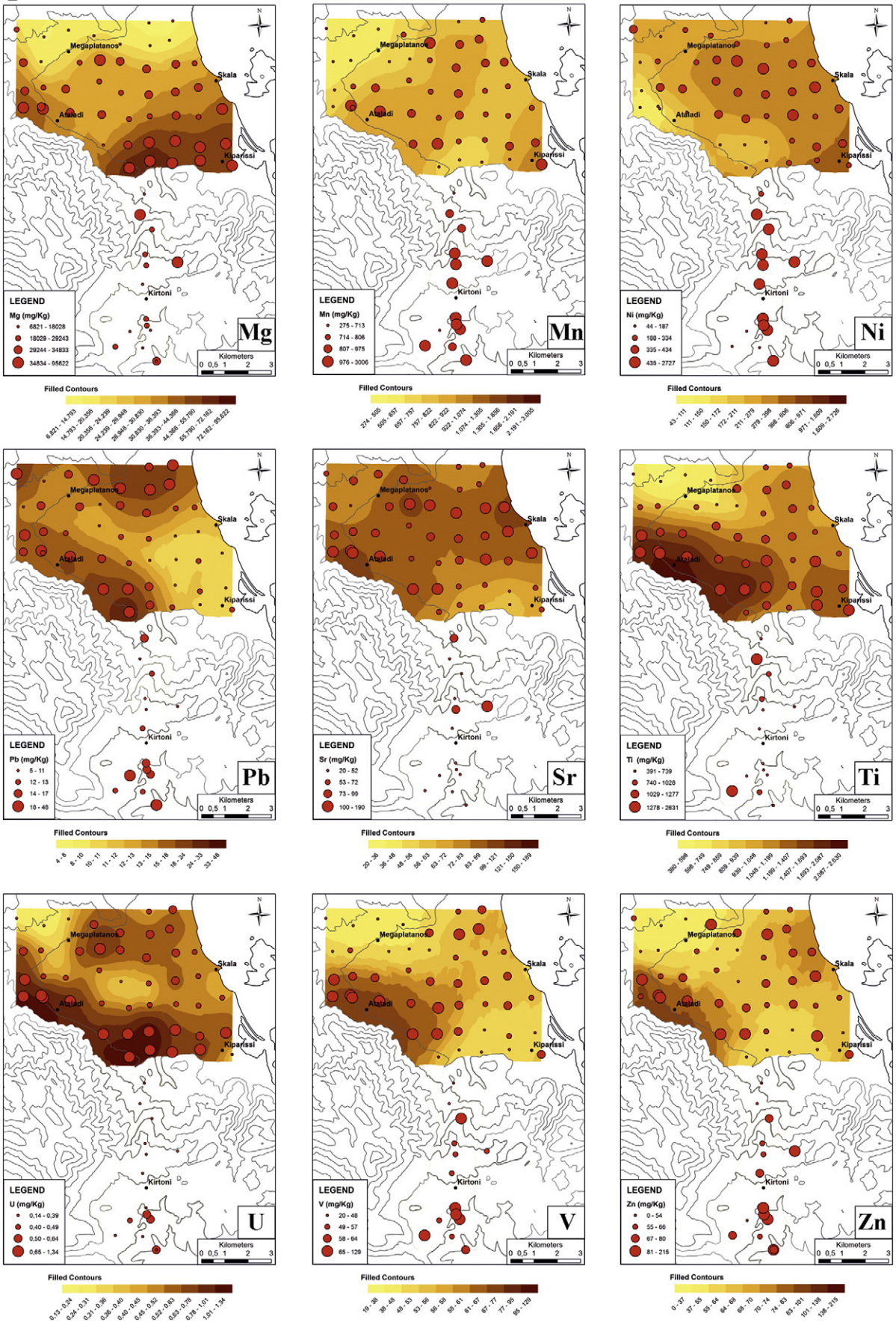

Fig. 4 (*continued*).

Table 4
Concentrations of selected elements and physicochemical parameters of groundwater samples.

Sample	Co	Cr	Mn	Ni	Fe	Mg^{+2}	Ca^{+2}	Na^{+}	K^{+}	SO_4^{-2}	Cl^{-}	HCO_3^{-}	NO_3^{-}	pH	TDS
	μg/L	μg/L	μg/L	μg/L	μg/L	mg/L	mg/L	mg/L	mg/L	mg/L	mg/L	mg/L	mg/L		g/L
AT-1	1.4	bdl	1	1	270	41.3	49	35	5	16	23.6	312	35.2	7.36	0.26
AT-2	0.8	4	bdl	2	13	40.4	54	34	6	15	40	285	36.1	7.45	0.31
AT-3	0.3	12	1	bdl	4	44.7	45	36	5	3	34	300	23.3	7.17	0.35
AT-4	0.7	23	3	bdl	6	57.7	73	37	6	36	68	287	144	7.17	0.49
AT-5	bdl	6	5	bdl	4	58.3	76.2	39	9	62	75.2	370	101	7.66	0.56
AT-6	bdl	25	5	2	6	55.1	70.4	31	11	64	63.6	293	113	7.74	0.54
AT-7	bdl	13	bdl	bdl	5	60.3	69.1	31	8	54	61.6	360	114	7.8	0.54
AT-8	bdl	2	bdl	bdl	3	41.1	42.4	20	3	8	30.8	360	7.5	7.88	0.32
AT-9	bdl	3	2	2	3	39.7	33.2	23	3	18	21.1	308	25.1	8.27	0.36
AT-10	bdl	3	3	5	4	37.2	32.6	21	4	15	50.4	262	35.2	8.22	0.36
KL-1	bdl	2	bdl	15	3	17.1	106	30	8	64	24.5	308	144	7.83	0.49
KL-2	bdl	2	bdl	2	5	29.2	71.4	18	4	33	17.7	273	77.4	7.89	0.37
KL-4	bdl	2	bdl	2	14	17	85.4	17	3	51	14.1	244	96.8	7.77	0.38

bdl = below detection limit.

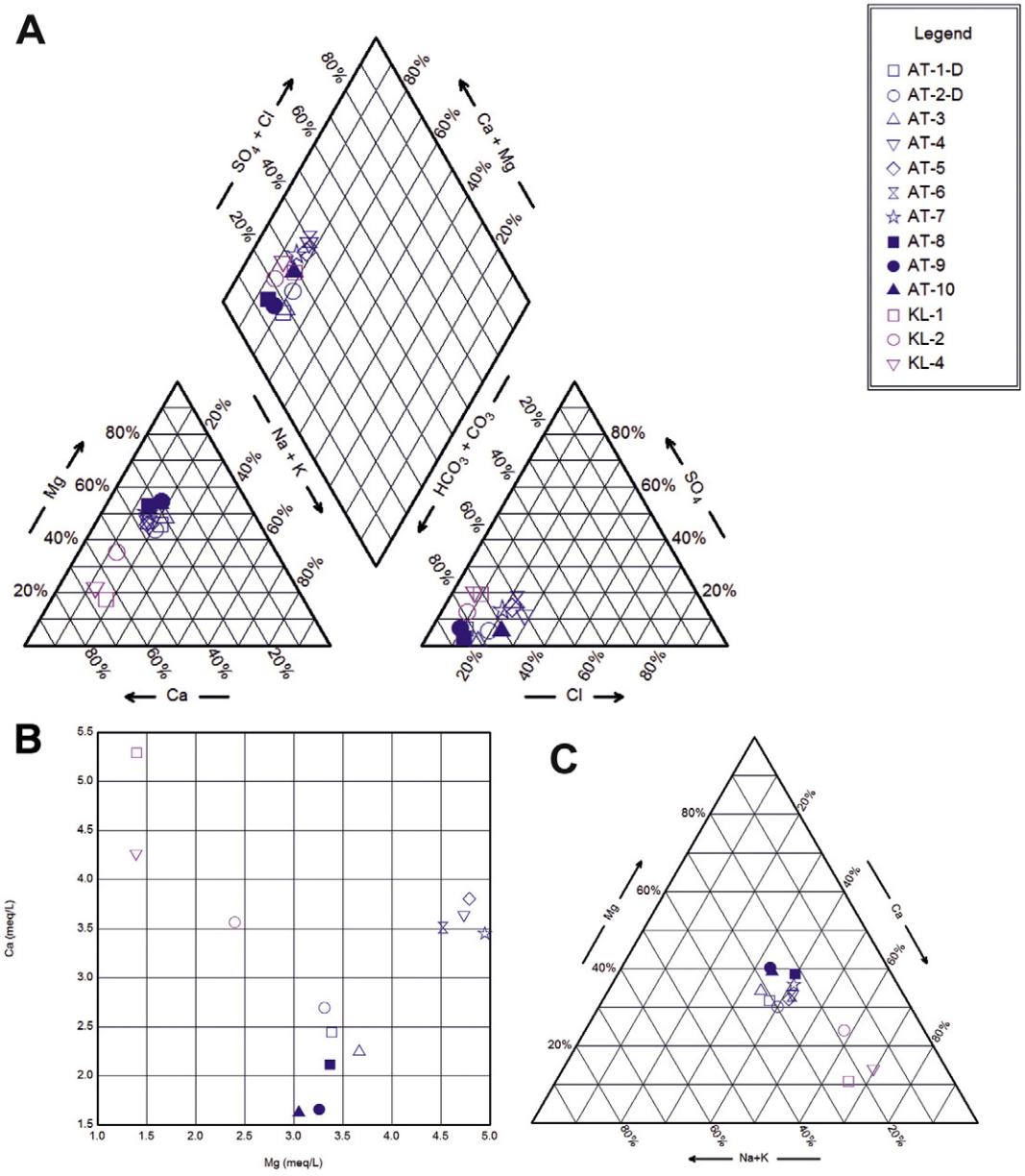

Fig. 5. (A) Chemical composition of groundwater samples plotted in Piper diagram. (B) Ca–Mg diagram presenting the chemical composition of groundwater samples. (C) Ca–Mg–Na + K ternary diagram presenting the chemical composition of groundwater samples.

5. Discussion

5.1. Soil baseline values and toposequence profiles of ophiolite derived elements

Based on the combined geochemical, mineralogical and statistical data, the spatial distribution of the elements and especially their correlation with lithological variability the total studied area was divided into two sub-areas of similar soil geochemical characteristics, as it is proposed for areas with different geochemical characteristics (Kanellopoulos and Argyraki, 2013). The elements that display the highest variation in their median values between the total area and the defined sub-groups of distinctive geology, i.e., near ultramafic rock occurrences in the Kirtoni area and the alluvial Valley of Atalanti, are Ca, Fe, Co, Cr, Ni, and Ti. Baseline values within the two sub-areas are expressed with the median values representing the typical elemental concentration in the studied sub-areas. The influence of ultramafic rocks outcropping in Kirtoni area is reflected on the elevated baseline concentrations of three typical ophiolite derived trace elements, i.e., Co, Ni and Cr. With respect to major elements, Ca and Mg are enriched in alluvial soil indicating the influence of dolomite rocks surrounding the valley.

The calculation of the upper limit of the baseline, i.e., threshold values, was based on the inflection point on the cumulative frequency curve of statistical distributions of elemental concentrations (Reimann et al., 2005). In general, concentration values that failed to fit on a linear regression model, thus representing values exceeding the threshold, were always over the 90th percentile (Table 2). Since the method does not involve any mathematical modification of the data, it provides an objective and reproducible way of calculating baselines when the data do not follow a normal distribution (Sierra et al., 2007).

Comparisons of measured concentrations of the ophiolite derived elements with those from other areas are highly influenced by the analytical method used. It has been already noted that the perchloric–nitric–hydrochloric acid attack used in the present study is a partial extraction method and is not very effective on spinels (e.g., chromite) or ilmenite, leading to underestimation of total Cr, Ti, V and other resistant mineral associated elements. Good examples of the magnitude of differences in elemental concentrations depending on the analytical method are provided byCr concentration measurements in the GEMAS project on agricultural and grazing land soil of Europe (Albanese et al., 2015) and the geochemical mapping project in Cyprus (Cohen et al., 2012).

The present study focuses on soil geochemistry of an ophiolite area, therefore the results are compared to existing datasets from other areas with similar geology. Recent research in the neighboring geographical area of northern Euboea Island where ultramafic rocks also occur indicated similar, although somehow lower concentrations of ophiolite derived elements (Kanellopoulos and Argyraki, 2013). These differences are attributed to the limited exposure of unweathered ultramafic rock in Euboea. Comparison of the results of the present study with those reported for the serpentine soils of Vergina (northern Greece) (Dermatas et al., 2014), an area rich in ultramafic rocks, indicates relative lower concentrations. However, the observed differences are affected by the different analytical method used as the total concentrations have been measured in Vergina by XRF. Also, compared to the extensive soil geochemical dataset of Cyprus which contains a large number of samples from across the Troodos ophiolite (ultramafics, mafic intrusives, mafic extrusives), the Kirtoni sample geochemistry is similar to the Troodos ultramafics except that Kirtoni is higher in Ti concentrations (Cohen et al., 2012) despite the near total dissolution used in the present study.

The concentration profiles of Cr, Ni and Co along the two topographical sections marked in Fig. 1 are presented in Fig. 6.

The concentration patterns of all three elements along topography are similar, however, some differences are noted between the two toposequences. An abrupt decline in soil elemental content is observed along the steep slope from Kirtoni towards the alluvial valley, leveling out on the flat topography towards the north of the section. In the second toposequence, which is characterized by a gentle slope, there is no much difference between concentrations along the section. Although ultramafic rocks outcrop on the shoulder of both toposequences, they differ on the degree of weathering and serpentinization. Specifically, the healthy peridotite present on high topography of the south–north section gives rise to much higher concentrations of Cr, Ni and Co than the intensively serpentinized rock on the west end of sections F–G (Fig. 1). The size and shape of the Cr-bearing soil grains are indicative of an early stage of moderate weathering intensity in the Kirtoni area. Soil within the valley is mechanically supplied with weathered material from the surrounding rock formations outcropping on the periphery of

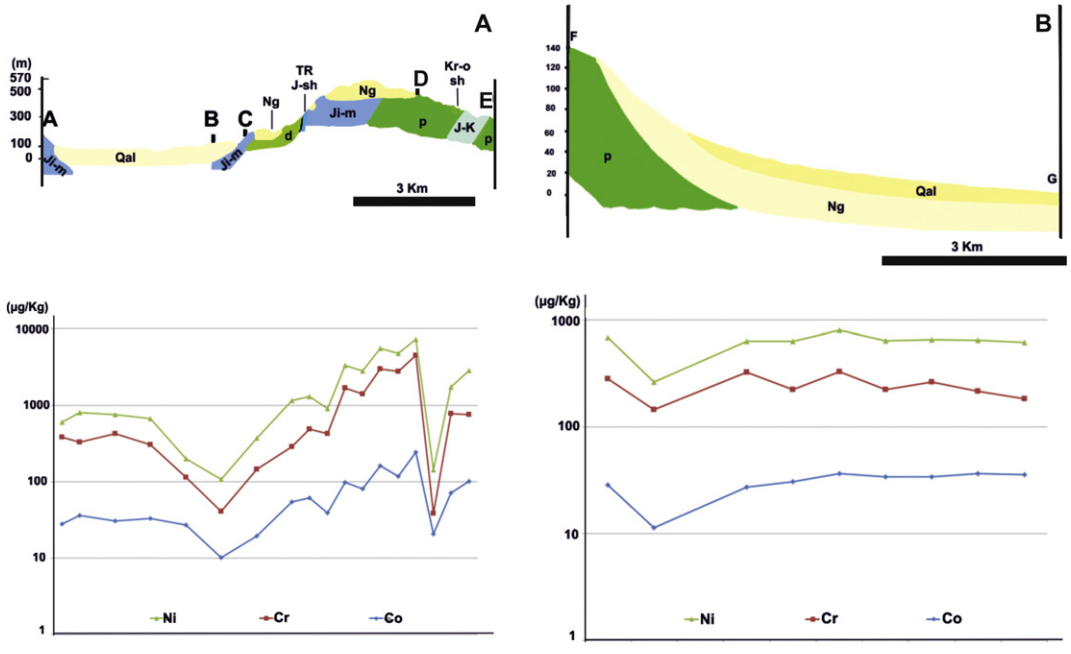

Fig. 6. Geological cross-sections and the related change of Ni, Cr and Co concentrations in topsoil (for the abbreviations of the geological formations see legend of Fig. 1).

the study area. In this instance, the size of Cr-bearing grains and minerals is quite smaller and their shape is more rounded (Fig. 2A, B) while no angular grains of chromite were observed.

Also, although no Ni-bearing phases were identified in the soil samples, the correlation coefficient between Cr and Ni declines from 0.91 ($p < 0.05$) in Kirtoni area to 0.56 ($p < 0.05$) in Atalanti Valley (Table 3). This is indicative of a change in the hosting phases of the two elements within the two areas. As the chemical weathering advances, Ni is usually accommodated in clay minerals e.g., smectite, while Cr remains in primary phases such as chromite (Cheng et al., 2011). This has been previously reported in a study of ultramafic affected soil in Thiva Greece (Kelepertzis et al., 2013). In general, because alluvial soil in the study area contains the weathering products of the surrounding outcropping ultramafic rocks, the fraction of related trace elements which is mobilized during pedogenic processes related to mineral dissolution, redox reactions and formation of secondary minerals varies depending on elemental speciation in soil.

The significant difference in soil Ni concentrations between the Kirtoni and Atalanti areas also gives rise to differences in the flora of the two areas. The Ni hyperaccumulator species *Alyssum chalcidicum* Janka (synonym *Alyssum murale* Waldst. & Kit) has been identified only in the area of Kirtoni (Kanellopoulos, 2011). The measured Ni concentration in the leaves of the plant was 2910 mg/kg indicating an enrichment factor of 2.3 over the average Ni concentration in the soil samples from the same area. This is a characteristic example that demonstrates the relationship between soil geochemistry and metal uptake by plants in the study area. In the Balkans, high concentrations of Ni can be found in soils derived from ultramafic rocks, causing hyperaccumulation of Ni to concentrations above 1000 mg/kg on some plant species like *A. murale* (Brooks, 2000; Bani et al., 2010; Reeves and Adiguzel, 2008).

Comparison of elemental concentrations between the two soil horizons (depth 0–25 cm and 25–50 cm) could provide an indication of relative enrichment or depletion of specific elements in the uppermost soil layer. However, the usefulness of such comparison is limited in providing proof of contamination by anthropogenic sources as a high value in the top/bottom-ratio may be related to other factors (Reimann and Garrett, 2005), e.g., increased content of organic matter in the top layer andhomogenization due to agricultural activities (i.e., plowing). In the present study this comparison indicated no significant differences between the two soil horizons (Fig. 3A).

5.2. Elemental interactions in the bedrock–soil–water system

The study of the groundwater samples indicated slight differences in the chemistry of the two distinct aquifers within the study area, i.e., the aquifer developing within the alluvial sediments of Atalanti Valley (magnesium-bicarbonate water type) and the aquifer developing within a small occurrence of Neogene deposits including gravels of unweathered ultramafic rocks and limestone from the neighboring occurrences in Kirtoni (calcium-bicarbonate water type).

Our discussion focuses on Cr because of the significance of this element for the environment. The water samples from Atalanti are enriched in Cr with concentrations from 5 up to 25 μg/L, depending on their spatial distribution within the alluvial plain. Specifically, five samples (AT 4–AT 7) situated along the central E–W axis of the alluvial plain present the highest Cr concentration values. This observation indicates that there is a relationship between the thickness of alluvial sediments, which are presumably thicker in the central part of the basin, and the Cr releasing process taking place during the water–soil–rock interaction. Notably, these water samples are also the most enriched in Mg. In contrast water samples located on the periphery of the basin show lower concentrations of Cr and Mg. Bearing in mind the geogenic source of Cr in the area the data indicate that the releasing process of this PHE within the shallow alluvial aquifer is conditioned by the geometry of the basin and subsequently by the groundwater flow and residence time. Chromium mobilization and groundwater enrichment in ophiolite related aquifers has been attributed by several authors to the oxidative action of Mn oxides as well as the alkaline water pH (Chardot et al., 2007; Cheng et al., 2011; Dermatas et al., 2014; Fandeur et al., 2009; Hseu and Iizuka, 2013). The process requires oxidation of Cr(III) present in primary minerals to Cr(VI) by Mn-oxides. The subsequent release of Cr into the groundwater is controlled by adsorption reactions on the surface of Mn and Fe-oxides (Fandeur et al., 2009). Other authors have suggested a potential role of different electron acceptors and complex mineral phases such as layered double hydroxides and hydroxycarbonates in geogenic Cr oxidation and release from the solid phase under Mediterranean climate conditions (Langone et al., 2013). Further work is required to better understand the release processes of Cr in groundwater, nevertheless the study area provides an interesting case for such studies.

Nickel concentrations in groundwater were significantly lower than Cr, especially in the alluvial aquifer of Atalanti. Primary silicate minerals containing Ni in ultramafic rocks are relatively unstable in the surface environment, releasing Ni which is subsequently incorporated into secondary clay minerals and Fe–Mn oxides. No Ni-bearing phases were identified in this study, however, the alkaline character of the alluvial soil (pH ~ 8) indicates that Ni is retained in solid phases similarly with observations from other ophiolite related areas in Greece (Kelepertzis et al., 2013). Water samples located near the coast are also influenced by sea water while the effect of anthropogenic activities e.g., extensive use of fertilizers and pesticides has also been demonstrated in the area by studying relevant water parameters (Kanellopoulos et al., 2014).

6. Conclusions

The agricultural soil of the studied valley is affected by the physical and chemical weathering of mafic and ultramafic rocks outcropping in the surrounding mountainous area, giving rise to elevated concentrations of Cr, Ni, Co and other elements. The supply of material in the valley is mainly achieved through the drainage network. In the uphill area of Kirtoni, the influence of relatively unweathered ultramafic rocks on the mineralogy and geochemistry of soil is dominant giving rise to maximum concentrations of Cr, Ni and Co in soil. The Ni hyperaccumulator species *Alyssum chalcidicum* was identified only in the area of Kirtoni, in close proximity to unweathered peridotite rock.

Different mobilization processes give rise to different groundwater concentrations of Cr and Ni in the alluvial aquifer of Atalanti plain. The relatively higher Cr mobilization and groundwater enrichment in the central axis of the alluvial aquifer is related to the increased thickness of sediment column and groundwater flow, allowing for effective water–soil–rock interaction and release into the water. Nickel is effectively retained in the solid phase under the prevailing alkaline soil conditions and has minimal concentrations in groundwater.

The results of this study can be utilized in future research at areas of similar geology and climatic conditions by providing an objective basis for setting realistic threshold values for pollution assessment and remediation.

Supplementary data to this article can be found online at http://dx.doi.org/10.1016/j.gexplo.2015.06.013.

Acknowledgments

The corresponding author would like to thank Professor Eugenia Valsami-Jones of the University of Birmingham, School of Geography, Earth and Environmental Sciences for her support and for giving him the opportunity to use the analytical facilities of the Natural History Museum of London. Also, he would like to thank Assistant Professor Lemonia Koumpli-Sobatsi of the University of Athens, Department of Biology for species identification of the vegetation samples. The two anonymous reviewers and Associate Editor Alecos Demetriades are acknowledged for their thorough review and useful comments and suggestions that greatly improved the quality of the paper.

References

Albanese, S., Sadeghi, M., Lima, A., Cicchella, D., Dinelli, E., Valera, P., Falconi, M., Demetriades, A., De Vivo, B., The GEMAS Project Team, 2015. GEMAS: cobalt, Cr, Cu and Ni distribution in agricultural and grazing land soil of Europe. J. Geochem. Explor. http://dx.doi.org/10.1016/j.gexplo.2015.01.004.

Bani, A., Pavlova, D., Echevarria, G., Mullaj, A., Reeves, R.D., Morel, J.L., Sulce, S., 2010. Nickel hyperaccumulation by the species of *Alyssum* and *Thlaspi* (Brassicaceae) from the ultramafic soils of the Balkans. Bot. Serbica 34, 3–14.

Brooks, R.R., 1987. Serpentine and its Vegetation. Dioscorides Press, Portland, OR.

Brooks, R., 2000. Plants That Hyperaccumulate Heavy Metals. CABI Publishing.

Chardot, V., Echevarria, G., Gury, M., Massoura, S., Morel, J.L., 2007. Nickel bioavailability in an ultramafic toposequence in the Vosges Mountains (France). Plant Soil 293, 7–21.

Cheng, C.-H., Jien, S.-H., Iizuka, Y., Tsai, H., Chang, Y.-H., Hseu, Z.-Y., 2011. Pedogenic chromium and nickel partitioning in serpentine soils along a toposequence. Soil Sci. Soc. Am. J. 75, 659–668.

Cohen, D., Rutherford, N., Morisseau, E., Zissimos, A., 2012. Geochemical patterns in the soils of Cyprus. Sci. Total Environ. 420, 250–262.

Cox, S.F., Chelliah, M.C.M., McKinley, J.M., Palmer, S., Ofterdinger, U., et al., 2013. The importance of solid-phase distribution on the oral bioaccessibility of Ni and Cr in soils overlying Palaeogene basalt lavas, Northern Ireland. Environ. Geochem. Health 35, 553–567.

Dermatas, D., Vatseris, C., Panagiotakis, I., Chrysochoou, M., 2012. Potential contribution of geogenic chromium in groundwater contamination of a Greek heavily industrialized area. Chemical Engineering Transactions 28. AIDIC (www.aidic.it/cet).

Dermatas, D., Mpouras, T., Chrysochoou, M., Panagiotakis, I., Vatseris, C., Linardos, N., Theologou, E., Boboti, N., Xenidis, A., Papassiopi, N., Sakellariou, L., 2014. Origin and concentration profile of chromium in a Greek aquifer. J. Hazard. Mater. 281, 35–46.

Economou-Eliopoulos, M., Megremi, I., Vasilatos, Ch., 2011. Factors controlling the heterogeneous distribution of Cr(VI) in soil, plants and groundwater: evidence from the Assopos basin, Greece. Chem. Erde 71, 39–52.

Fandeur, D., Juillot, F., Morin, G., Olivi, L., Cognigni, A., Webb, S.M., Ambrosi, J.-P., Fritsch, E., Guyot, F., Brown, G.E., 2009. XANES evidence for oxidation of Cr(III) to Cr(VI) by Mn-oxides in a lateritic regolith developed on serpentinized ultramafic rocks of New Caledonia. Environ. Sci. Technol. 43, 7384–7390.

Garnier, J., Quantin, C., Guimarães, E., Becquer, T., 2008. Can chromite weathering be a source of Cr in soils? Mineral. Mag. 72 (1), 49–53.

Garnier, J., Quantin, C., Guimaraes, E.M., Vantelon, D., Montarges-Pelletier, E., Becquer, T., 2013. Cr(VI) genesis and dynamics in Ferrasols developed from ultramafic rocks: the case of Niquelandia, Brasil. Geoderma 193–194, 256–264.

Garrels, R.M., 1968. Genesis of some ground waters from igneous rocks. In: Abelson, P.H. (Ed.), Researches in geochemistry 2. Wiley, pp. 406–420.

Gasser, U.G., Dahlgren, R.A., 1994. Solid-phase speciation and surface association of metals in serpentinitic soils. Soil Sci. 158, 409–420.

Gough, L.P., Meadows, G.R., Jackson, L.L., Dudka, S., 1989. Biogeochemistry of a highly serpentinized, chromite-rich ultramafic area, Tehama County, California. US Geol. Surv. Bull. 1901, 1–24.

Hseu, Z.-Y., Iizuka, Y., 2013. Pedogeochemical characteristics of chromite in a paddy soil derived from serpentinites. Geoderma 202–203, 126–133.

I.G.M.E., 1965. Atalanti Sheet, Geological Map 1:50,000. Department of Geological Maps of IGME, Athens.

Jolivet, L., Faccenna, C., Huet, B., Labrousse, L., Le Pourhiet, L., Lacombe, O., Lecomte, E., Burov, E., Denèle, Y., Brun, J.-P., Philippon, M., et al., 2013. Aegean tectonics: strain localisation, slab tearing and trench retreat. Tectonophysics 597–598, 1–33.

Kabata-Pendias, A., Mukherjee, A., 2007. Trace Elements From Soil to Human. Springer-Verlag, Berlin, New York.

Kanellopoulos C., 2011. Geochemical research on the distribution of metallic and other elements to the cold and thermal groundwater, soils and plants in Fthiotida Prefecture and N. Euboea. Environmental impact. Unpublished Ph.D. Thesis, University of Athens, Greece (in Greek).

Kanellopoulos, C., Argyraki, A., 2013. Soil baseline geochemistry and plant response in areas of complex geology. Application to NW Euboea, Greece. Chem. Erde-Geochem. 73 (4), 519–532.

Kanellopoulos, C., Mitropoulos, P., Argyraki, A., 2014. Geochemical effect of ultrabasic ophiolitic rock chemistry and anthropogenic activities on groundwater contamination: the case of Atalanti area, Greece. XX Congress of the Carpathian Balkan Geological Association. Bul. Shk. Gjeol. 2, pp. 329–332.

Kelepertzis, E., Stathopoulou, E., 2013. Availability of geogenic heavy metals in soils of Thiva town (central Greece). Environ. Monit. Assess. 185 (11), 9603–9618.

Kelepertzis, E., Galanos, E., Mitsis, I., 2013. Origin, mineral speciation and geochemical baseline mapping of Ni and Cr in agricultural top soils of Thiva Valley (Central Greece). J. Geochem. Explor. 125, 56–68.

Langone, A., Baneschi, I., Boschi, C., Dini, A., Guidi, M., Cavallo, A., 2013. Serpentinite–water interaction and chromium (VI) release in spring water: examples from Tuscan ophiolites. Ofioliti 38 (1), 41–57.

Megremi, I., 2010. Distribution and bioavailability of Cr in central Euboea, Greece. CEJ Geosci. 2 (2), 103–123.

Megremi, I., Vasilatos, Ch., Economou-Eliopoulos, M., Mitsis, I., 2012. On the Speciation and the Sources of Chromium in Groundwater in Eastern Sterea Hellas, Greece: Natural Versus Anthropogenic Origin. PRE.ORG, Protection and Restoration of the Environment XI, Thessaloniki.

Moraetis, D., Nikolaidis, N.P., Karatzas, G.P., Dokou, Z., Kalogerakis, N., et al., 2012. Origin and mobility of hexavalent chromium in North-Eastern Attica, Greece. Appl. Geochem. 27, 1170–1178.

Mountrakis, D., 1986. The Pelagonian zone in Greece: a polyphase deformed fragment of the Cimmerian continent and its role in the geotectonic evolution of the Eastern Mediterranean. J. Geol. 94, 335–347.

Oze, C., Fendorf, S.E., Bird, D.K., Coleman, R., 2004a. Chromium geochemistry of serpentine soils. Int. Geol. Rev. 46 (2), 97–126.

Oze, C., Fendorf, S.E., Bird, D.K., Coleman, R., 2004b. Chromium geochemistry in serpentinized ultramafic rocks and serpentine soils in the Franciscan Complex of California. Am. J. Sci. 304 (1), 67–101.

Oze, C., Skinner, C., Schroth, A., 2008. Growing up green on serpentine soils: biogeochemistry of serpentine vegetation in the Central Coast Range of California. Appl. Geochem. 23 (12), 3391–3403.

Pe-Piper, G., Piper, D., 2002. The Igneous Rocks of Greece, The Anatomy of an Orogen. Gebruder Borntraeger, Berlin.

Pomonis, P., 2015. Personal Communication.

Proctor, J., Nagy, L., 1992. Ultramafic rocks and their vegetation: an overview. In: Baker, A.J.M., Proctor, J., Reeves, R.D. (Eds.), The Vegetation of Ultramafic (Serpentine) Soils. Intercept, Handover, UK, pp. 469–494.

Ramsey, M.H., Thompson, M., Banerjee, E.K., 1987. A realistic assessment of analytical data quality from inductively coupled plasma atomic emission spectrometry. Anal. Proc. 24, 260–265.

Reeves, D., Adiguzel, N., 2008. The nickel hyperaccumulating plants of the serpentines of Turkey and adjacent areas: a review with new data. Turk. J. Biol. 32, 143–153.

Reimann, C., Garrett, R.G., 2005. Geochemical background – concept and reality. Sci. Total Environ. 350, 12–27.

Reimann, C., Filzmoser, P., Garrett, R.G., 2005. Background and threshold: critical comparison of methods of determination. Sci. Total Environ. 346, 1–16.

Reimann, C., Birke, M., Demetriades, A., Filzmoser, P., O'Connor, P. (Eds.), 2014. Chemistry of Europe's Agricultural Soils. PartA: Methodology and Interpretation of the GEMAS Data SetGeol. Jb., B 102. Geologisches Jahrbuch (Reihe B 102), Schweizerbarth, Hannover (528 pp.).

Sadegh, M.J.M., Ahmad Heidari, A., Sarmadian, F., 2012. The role of pedogenic processes and soil characteristics on nickel distribution in some Oxiaquic Paleudalfs. Int. Res. J. Appl. Basic Sci. 3 (5), 1032–1039.

Salminen, R., Batista, M.J., Bidovec, M., Demetriades, A., 2005. Geochemical Atlas of Europe. Part1: Background Information, Methodology and Maps. (http://weppi.gtk.fi/publ/foregsatlas).

Selinus, O., Alloway, B., Centeno, J.A., Finkelman, R.B., Fuge, R., Lindh, U., Smedley, P., 2005. Essentials of Medical Geology — Impacts of the Natural Environment on Public Health. Elsevier.

Sierra, M., Martinez, F.J., Aquilar, J., 2007. Baselines for trace elements and evaluation of environmental risk in soils of Almeria (SE Spain). Geoderma 139, 209–219.

Vardaki, C., Kelepertsis, A., 1999. Environmental impact of heavy metals (Fe, Ni, Cr, Co) in soils waters and plants of Triada in Euboea from ultrabasic rocks and nickeliferous mineralization. Environ. Geochem. Health 21, 211–226.